Varela, M.J., Ceccarelli, M., Flores, P., A kinematic characterization of human walking by using CaTraSys. Mechanism and Machine Theory, Vol. 86, pp. 125-139, 2015

A kinematic characterization of human walking by using CaTraSys

Maria João Varela[a], Marco Ceccarelli[b,*], Paulo Flores[a]

[a] CT2M/DSM Department of Mechanical Engineering, University of Minho
Azurém Campus, 4800-058 Guimarães, Portugal
Email: mariajoaovarelac@gmail.com; pflores@dem.uminho.pt

[b] LARM: Laboratory of Robotics and Mechatronics
DICeM, University of Cassino and South Latium
Via Di Biasio 43, 03043 Cassino (Fr), Italy
Email: ceccarelli@unicas.it

Abstract

This paper presents an experimental characterization of the biomechanics of human gait by means of Cassino Tracking System (CaTraSys). CaTraSys is a passive cable-based parallel manipulator that is used to determine pose and exerted force of mechanical systems along large trajectories. It is a low-cost easy-operable system that has been utilized in the present work for a clinical application as an assessing device for diagnosis and rehabilitation procedures. A methodology for experimental tests and data analysis is outlined, which includes mean extrapolation of acquired trajectory data. Basic characteristics of two-dimensional (2D) and three-dimensional (3D) resulting gait patterns are discussed. Using spatiotemporal parameters, different test conditions and anthropometric characteristics are evaluated in order to assess their influence on the human walking from the kinematic point of view.

Keywords: Biomechanics, Human gait, Experimental mechanics, CaTraSys

1. Introduction

It is known that the methods that are used in gait research frequently include pressure and force plates [1, 2], video or optoelectronic-based analysis systems [3], accelerometers, gyroscopes [4], instrumented shoes [5] and pressure and force sensitive footswitches [6, 7]. These systems are utilized to acquire kinematic and kinetic gait data, such as trajectories or ground reaction forces.

In the Robotics field, cable-based parallel manipulators have been considered to be interesting systems. This type of systems is cable actuated in which cables are connected to the end-effector from a stationary frame. They ensure very good kinematic and dynamic characteristics and are characterized by an easy set-up, transportability and good inertial behavior due to small moving masses consisting of cables and light end-effectors. Another important feature is that the calibration procedure must be performed when any component of the system is changed and periodically. A drawback associated with these robotic manipulators deals with the requirement of operating in a reduced

* Corresponding author: Telephone: +39-0776-2993663; Fax: +39-0776-2993989

workspace in order to avoid cables interference. The most important characteristics are the low cost and easy operation that can be considered very important for a possible commercial system [8, 9]. All these features are also suitable for clinical applications [10]. Besides allowing to record gait information, these manipulators can be utilized to guide movement of human limbs, which make them attractive even as rehabilitation devices. In addition, cable-based systems can be reconfigured for different therapies. The cables in opposition to the rigid links reduce the constraints [8, 9, 11].

CaTraSys [12] is a passive cable-based parallel manipulator with possible application in clinical fields as an assessing device. Experimental tests of a patient limb performance could give the clinicians information towards diagnosis and rehabilitation procedures. Iida and Yamamuro [13] studied patients performance before and after joint replacement, and they observed that the 3D displacements curves of the body centre of gravity that were initially distorted, tended to normalize after the clinical procedure. These results can be seen as a proof of the clinical potential of CaTraSys. Thus, the purpose of the present work deals with the experimental characterization of human gait using CaTraSys. In this process, the mean trajectory pattern of the gait tests is evaluated and a kinematic analysis is carried out from experimental acquired data. Four different test settings and anthropometric features are evaluated utilizing spatiotemporal parameters.

2. CaTraSys for motion tracking

CaTraSys, presented in Fig. 1a, was developed at the Laboratory of Robotics and Mechatronics (LARM), Department of Civil and Mechanical Engineering (DICeM) of the University of Cassino and South Latium, in 1993. Since then it has been continuously evolved in operation and design and it has been successfully utilized in different applications for determination of workspace, kinematic parameters and force exerted by robots and human limbs [12]. CaTraSys is constituted by mechanical and electronic components together with a software package, as it is illustrated in Fig. 1b. The Trilateral Sensing Platform (TSP) is constituted by a metal stationary platform on which are fixed six position sensors T_i (i=1…6) (cable extension transducers celesco™ PT101 [14]) and six force sensors C_i (i=1…6) (tension/compression load cells LAUMAS® SA [15]). Each cable is attached to a spring of a position sensor, such that it is conducted through the pair of pulleys and finally reaches the end-effector structure (see Fig. 2). The moving platform is the end-effector for CaTraSys and allows the system to track the movement. Pose of the end-effector and tension applied to pull it are determined through the position and force sensors, respectively.

The signals from the position and force sensors are conducted to the six amplifiers A_i (i=1…6) (analog weight transmitters LAUMAS® TPS [16]), which provide signal amplification. Then, a data acquisition (DAQ) board (National Instruments™ USB-6210 [17]) and the software packages Laboratory Virtual Instrument Engineering Workbench (LabVIEW™) and MATrix LABoratory (MATLAB®) are utilized for the purpose of data acquisition and data processing. The voltage is provided by a direct current (DC) power supply [18]. The springs and pulleys contribute to maintain the tension of the cables. The tension has a range limit since, on one hand, they need a minimum value to avoid its slackness and, on the other hand, a maximum value to minimize elastic and inelastic effects [8]. The pulleys are considered with the purpose of obtaining a compact system where the cables can move in a relatively large range, without the risk of cable folding, wrapping or damaging [18].

In the present work, regarding the moving platform, six steel cables are utilized in a 3-3 configuration, as it is illustrated in Fig. 3a. End-effectors are tightly strapped to the legs around two measurement points, namely at the medium line of the knee and close to the ankle. The proper positioning at the location of interest is ensured by Velcro® custom straps, which are soft, flexible and adaptable. However, the straps can be source of some inaccuracy in the measurements. It is important to note that CaTraSys formulation considers knee and ankle end-effectors as two points moving in the workspace (see points *K* and *A* in Fig. 3a).

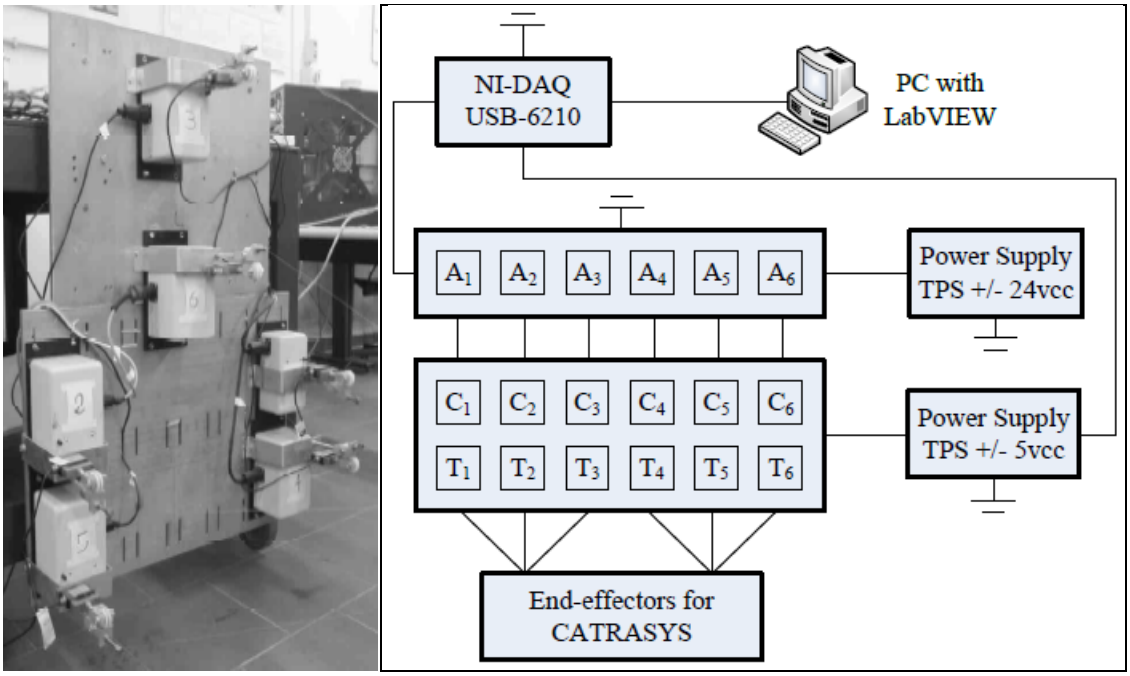

(a) (b)

Figure 1 - (a) Photography of the CaTraSys prototype; (b) Schematic representation of CaTraSys components [18].

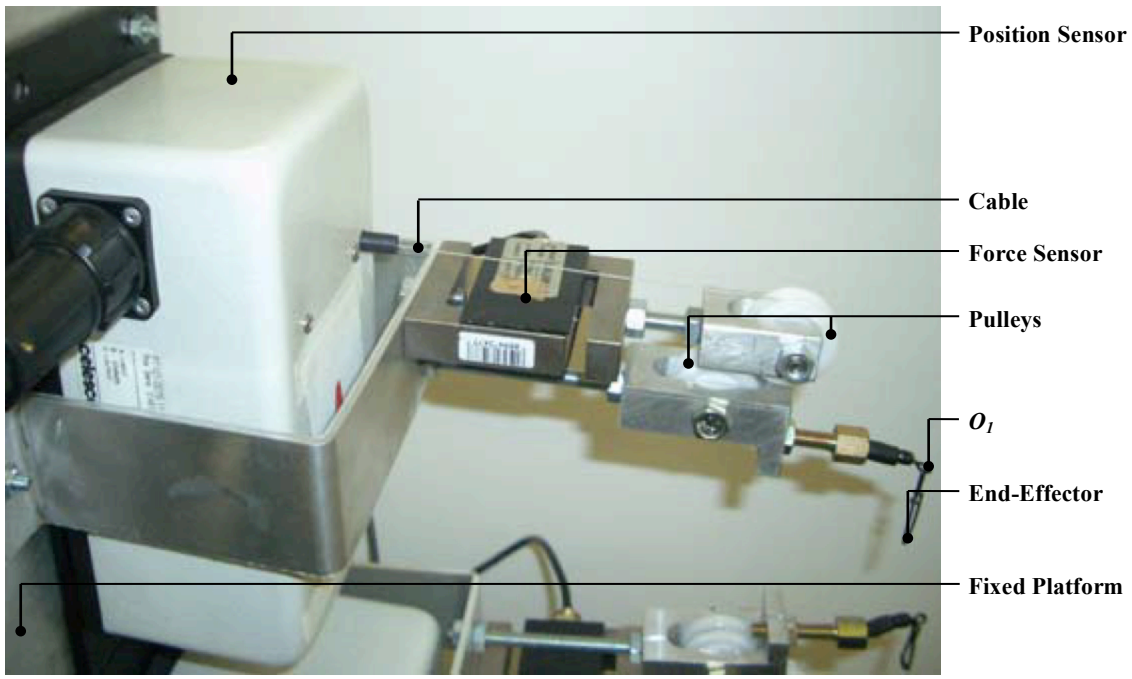

Figure 2 - Installation of CaTraSys components.

CaTraSys can be modeled as a six degrees-of-freedom (DOFs) parallel manipulator since cables can be considered as extensible legs connecting the platform and base by means of spherical and universal joints, respectively. CaTraSys is a passive cable system since the input motion is given through the action on the end-effector. The system can be used to identify the six DOFs of a body in space, being capable to give 3D pose (position and orientation) and force information [8].

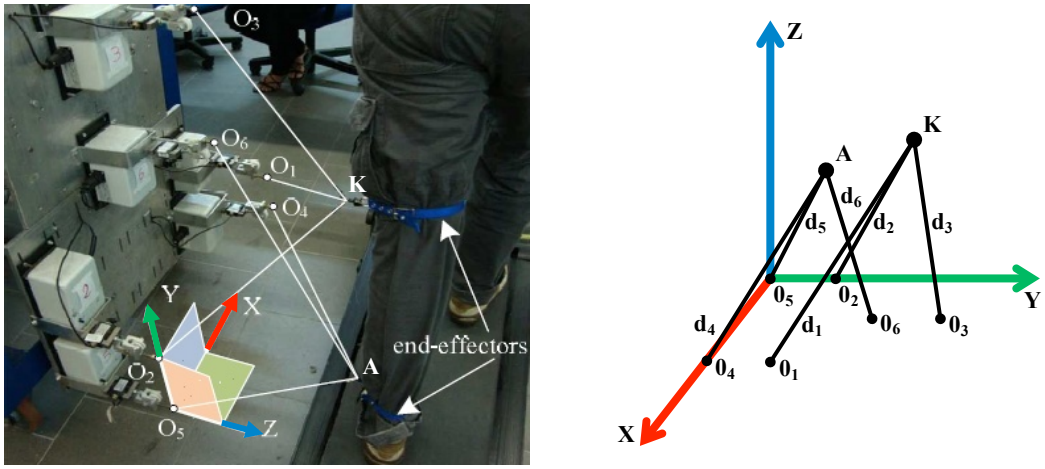

(a) (b)

Figure 3 - CaTraSys 3-3 configuration: (a) A treadmill gait assessment in which the end-effectors are strapped to the knee and ankle {adapted from [18]}; (b) A corresponding trilateration scheme.

The main objective of CaTraSys developments is to combine the low-cost, the easy-operability and the mechanical robustness features. It is considered a low-cost system when compared to other available commercial measuring systems, such as video capture systems. This is possible because CaTraSys only uses commercial off-the-shelf mechanical components, which makes it an economical and robust system. The intuitive and fast operation of CaTraSys is due to the simplicity of the trilateration method, which is the base of determining pose of the moving platform, and to the simple calibration. In addition, CaTraSys works in real-time allowing for the immediate evaluation of the test results [12]. CaTraSys is also very adaptable to different robotic schemes. The parallel architecture of CaTraSys moving platform can be utilized in diverse configurations, i.e., different number of end-effectors and cables. Additional relevant features of CaTraSys are the following, the position of the sensors in the stationary platform can be changed, the system can be used along with other measurement instruments, different rigid mechanical systems can be easily attached and movements can be performed in different planes [8].

The Virtual Instrument (VI) uses the DAQ software to collect, at a sample rate of 40 Hz, and calibrate the length and force data. The formula node does the trilateration and forces computations, of which result the knee and ankle trajectory as well as the force components (total of six positions and six forces).

Figure 3b depicts the trilateration scheme corresponding to the CaTraSys walking test of Fig. 3a. Cables one, two and three are attached to the knee point K and cables four, five and six are connected to the ankle point A. Points O_1, O_2 and O_3 are the base points of the cables, while d_1, d_2 and d_3 represent the distance between points K and O_1, O_2 and O_3. With the purpose of determining the coordinates of a point it is necessary, at least, to know the location of three fixed points together with three distances, which, in this work, are measured by the position sensors. In short, if at a specific instant of time, the coordinates of points O_1, O_2 and O_3 and the distances d_1, d_2

and d_3 are defined, it is possible to solve the system of equations of the trilateration technique. The distances d_1, d_2 and d_3 can be seen as radii of spheres, whose intersection identifies the location of point K and whose center points are the known O_1, O_2 and O_3. This is the basis of the 3D trilateration.

With regard to Fig. 3b and by using the algebraic manipulation of the trilateration technique for the knee K, it is possible to write the following expressions

$$d_1^2 - d_2^2 = (x - x_1)^2 - (x - x_2)^2 + (y - y_1)^2 - (y - y_2)^2 + (z - z_1)^2 - (z - z_2)^2 \quad (1)$$

$$d_2^2 - d_3^2 = (x - x_2)^2 - (x - x_3)^2 + (y - y_2)^2 - (y - y_3)^2 + (z - z_2)^2 - (z - z_3)^2 \quad (2)$$

where $K = (x, y, z)$ and $O_i = (x_i, y_i, z_i)$, for $i = 1, 2, 3$.

Solving Equations (1) and (2), the coordinates of K can be expressed as

$$x = H_x z + E_x \quad (3)$$

$$y = H_y z + E_y \quad (4)$$

$$z = \frac{-B_2 - \sqrt{B_2^2 - 4B_1B_3}}{2B_1} \quad (5)$$

where

$$A_i = d_i^2 - x_i^2 - y_i^2 - z_i^2 \quad (6)$$

$$X_{ij} = 2(x_i - x_j) \quad (7)$$

$$Y_{ij} = 2(y_i - y_j) \quad (8)$$

$$Z_{ij} = 2(z_i - z_j), \text{ for } i, j = 1, 2, 3 \quad (9)$$

$$x = \frac{A_1 - A_2 - Y_{21}y - Z_{21}z}{X_{21}} \quad (10)$$

$$H_y = \frac{X_{32}Z_{21} - X_{21}Z_{32}}{X_{21}Y_{32} - X_{32}Y_{21}} \quad (11)$$

$$E_y = \frac{-A_1X_{32} + A_2(X_{21} + X_{32}) - A_3X_{21}}{X_{21}Y_{32} - X_{32}Y_{21}} \quad (12)$$

$$H_x = \frac{-Y_{21}H_y - Z_{21}}{X_{21}} \quad (13)$$

$$E_x = \frac{A_1 - A_2 - Y_{21}E_y}{X_{21}} \quad (14)$$

$$B_1 = H_x^2 + H_y^2 + 1 \quad (15)$$

$$B_2 = 2H_x(E_x - x_3) + 2H_y(E_y - y_3) - 2z_3 \quad (16)$$

$$B_3 = E_x^2 + E_y^2 - A_3 - 2E_x x_3 - 2E_y y_3 \quad (17)$$

This approach can be applied to the ankle point A. Thus, in a similar way, the shank segment K to A is tracked while the end-effectors move during the experimental test.

3. Experimental procedures and data collection

The experimental test rig used in this work was constructed and operated at the LARM, which combines a non-motorized treadmill with an angle of incline of 7.3° and positioned parallel to CaTraSys fixed platform. In total, eight healthy subjects (5 male, 3 female; age 24.8±3.6 years old; height 1.683±0.077 m; weight 62.3±9.6 kg; shoe size

39.6±2.5; mean±standard deviation) from the University community volunteered to perform tests in this research.

The first gait assessment task was recorded with a subject walking at a self-selected velocity, with an average value of 4 km/h, and has been named as reference test. Then, in the loading test, an individual was tested when wearing a 6 kg backpack on his shoulders and centered on the back. In the next condition, a subject stepped out of the treadmill, changed his shoes and performed the footwear test. At last, a participant walked with a higher velocity but without running, being the estimated velocity equal to 6 km/h. This scenario was denominated as fast test.

With the purpose of having a standard dressing protocol, it was established participants to wear shorts and light casual shoes, i.e., not sportive, high heel, or open toes shoes (in-shoe assessment), as it is shown in Fig. 4a. In the footwear test a particular type of shoes was demanded. Men were required to wear sport shoes type (see Fig. 4b) and women used a specific high heel shoes with 74 cm of heel (see Fig. 4c).

(a) (b) (c)

Figure 4 - Footwear types used for experimental tests: (a) Casual shoes; (b) Sport shoes; (c) High heel shoes.

It must be highlighted that each individual performed four gait tests on two different days while supervised by the same operator. Data of the left hand side for 10 consecutive steady strides of forward walking was recorded per test [19].

It is known that any signal, when sampled at an adequate rate, can be expressed as series of sine and cosine waveforms of variable frequency [20]. Furthermore, Butterworth digital filter produces a smoother signal and is commonly used to process biomechanical data [21]. A low-pass fourth order zero-lag Butterworth filter was considered, with a range of cut-off frequencies between 2 and 4 Hz, which were applied to different tracked points and component directions. Besides, pre-processing of the signals was provided, and in some cases filtering after the data processing was also required. In order to determine the mean trajectory data over multiple gait cycles two assumptions were made, namely, the gait cycles are periodic and the time normalization to 0-100% of gait cycle refers to consecutive ipsilateral heel-strikes.

In order to identify the individual test data and taking into account the intra-variability associated with gait, it was first necessary to pre-analyze and select between the two experimental sessions. The fundamental idea was to select the experimental data in which the plot of the ankle sagittal trajectory is less disperse (see Fig. 5) so that reproducible mean data could be obtained.

The next step deals with the determination of the mean pattern of knee and ankle plots. In what follows, an explanation on the adopted procedure is presented for the ankle trajectory case. For this purpose, let consider the plot of Fig. 6a relative to the ankle horizontal trajectory. Each peak is labeled with a black circle that identifies the beginning of a gait cycle, corresponding to the heel-strike instant. Thus, the developed algorithm started by detecting these peaks. Even after the pre-filtering, some signals presented very small glitches at the spikes (see Fig. 6b). It should be noticed that these local maximums were initially tracked by the algorithm, and some difficulties in the

location of the global maximums points could be found. Therefore, the strategy adopted here was not to fix the glitches, but instead it skips those, i.e., when a peak close to the previous one was found, it was not initiated a new cycle. In order to define the walking time, the first and last peaks were neglected which is a procedure used in in-shoe systems, as it is illustrated in Fig. 6c [22]. After obtaining information on the correct and acceptable peaks index, the detection of those indexes was possible on the remaining directions of motion.

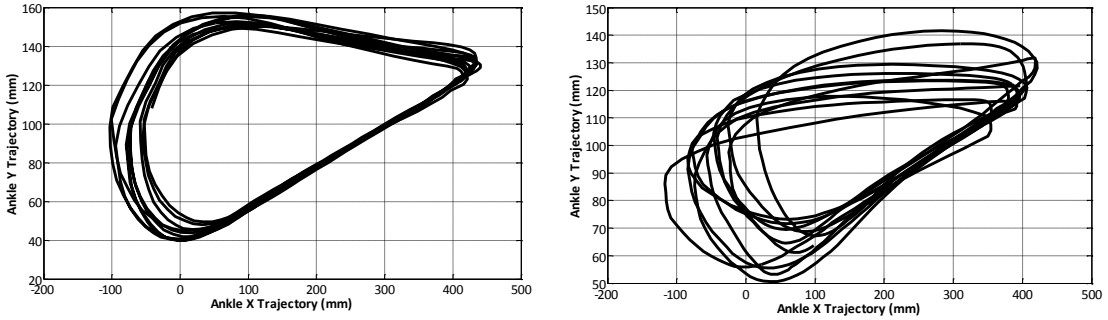

(a) (b)

Figure 5 - Results of two experimental tests in sagittal plane: (a) Data with acceptable dispersion; (b) Rejected data.

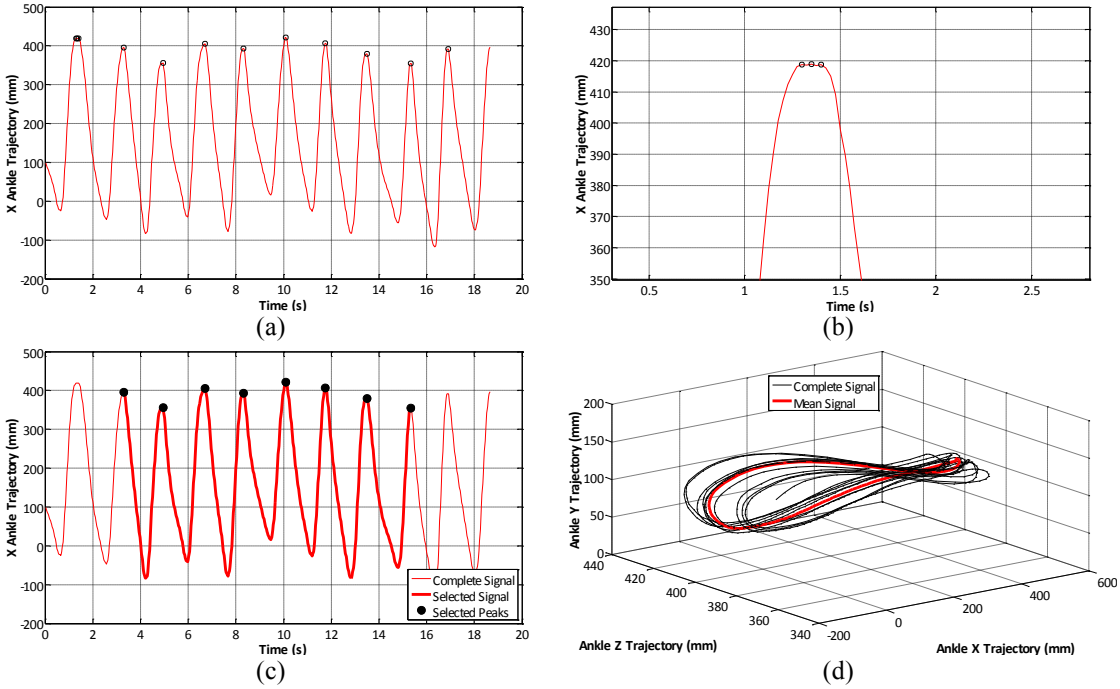

(a) (b) (c) (d)

Figure 6 – Treatment analysis: (a) Local and global maximums of the horizontal trajectory; (b) Zoomed view; (c) Final selected peaks; (d) Original and mean curves.

After finding the peaks, the developed algorithm read and treated the data between each pair of peaks, i.e., cycle by cycle. For averaging purposes, the time normalization of each cycle was needed, where each cycle was normalized to 100 points through a spline interpolation. The time variability of the gait cycles involves different amount of data per cycle, and therefore it was necessary to interpolate each cycle in order to allow the averaging across the number of cycles. Figure 6d shows the mean data and original plots obtained with this process.

In order to compute the shank angle θ_s during a gait cycle, the position data of knee and ankle was considered. From the Cartesian coordinates of the knee and ankle, it is possible to rewrite the following equation

$$\theta_s = tan^{-1} \frac{y_{knee} - y_{ankle}}{x_{knee} - x_{ankle}} \tag{18}$$

In turn, the velocity and acceleration were determined by using the finite-difference technique, yielding

$$v_{x_i} = \frac{x_{i+1} - x_{i-1}}{2\Delta t} \tag{19}$$

$$a_{x_i} = \frac{v_{x_{i+1}} - v_{x_{i-1}}}{2\Delta t} \tag{20}$$

where Δt defines the time step [21].

Gait parameters can be used to characterize the individual (or robotic) gait, to evaluate pathological gaits for example [23, 24], and also to reproduce human gait by applying these parameters with adequate software (Working Model, for example) or in humanoid robotics [23]. In the present work, an objective analysis to the inter-variability of the gait population was run. Each test result was quantified through spatiotemporal parameters, obtained using the complete and mean signal of the ankle trajectory (see Table 1).

Table 1 - Computation and physical meaning of the spatiotemporal parameters.

Spatiotemporal Parameters	**Computation**	**Physical Meaning**
Cycle Cadence (cycles/s)	Number of strides divided by walking time	Number of cycles per second
Stance Phase (%)	Percentage of cycle between the first position and the minimum position of the mean vertical signal	Percentage of cycle the foot spent on the treadmill
Swing Phase (%)	Percentage of cycle between the minimum and the last position of the mean vertical signal	Percentage of cycle the foot spent in the air
Cycle Height (m)	Difference between the minimum and maximum position of the mean vertical trajectory	Range of the foot vertical position
Cycle Length (m)	Difference between the minimum and maximum position of the mean horizontal trajectory [25]	Range of the foot horizontal position
Cycle Medio-Lateral Movement (m)	Difference between the highest and the lowest lateral mean position	Range of the foot lateral position

4. Results for a numerical characterization

Figures 7 and 8 show the mean trajectory of knee and ankle points, respectively. The oval and figure-of-eight shapes were generally found for all the subjects and types of gait tests. The arrows show the motion direction. The orange and purple ones depict the beginning of stance and swing phases, respectively. The first correspond to the time the foot is on the treadmill and the second to the time the foot is in the air. The presented 3D plots can be named as trajectory *cyclogram* and they provide spatial but not temporal information [26].

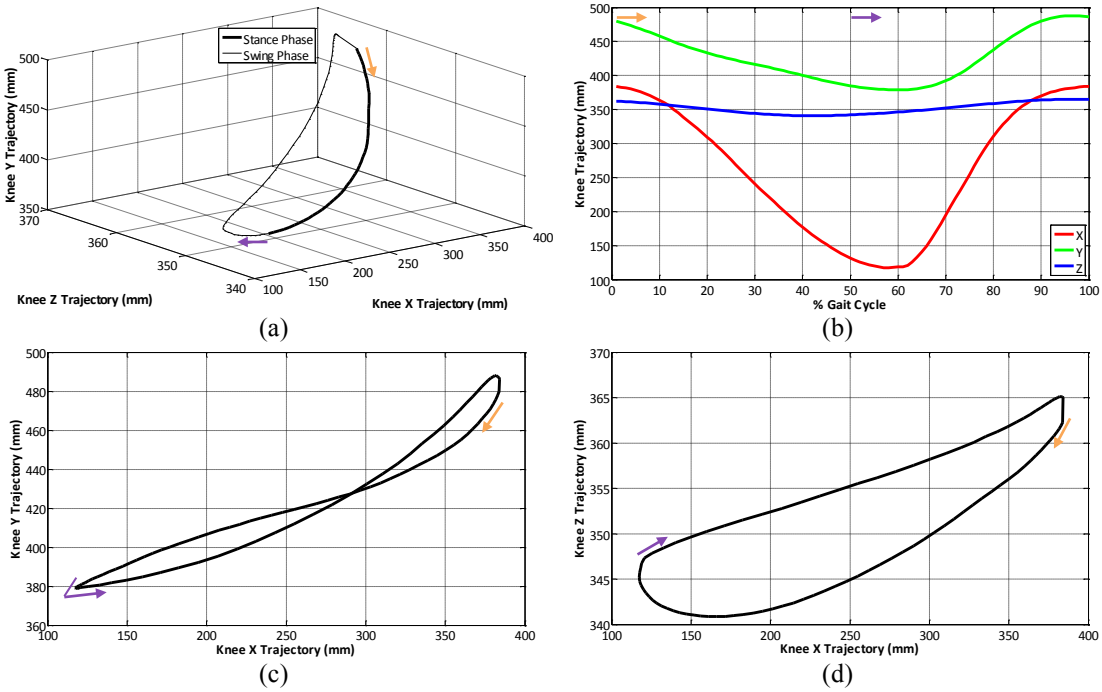

Figure 7 - Knee trajectory: (a) 3D; (b) *X*, *Y* and *Z* coordinates; (c) Sagittal plane; (d) Transverse plane. The arrows show the direction of motion.

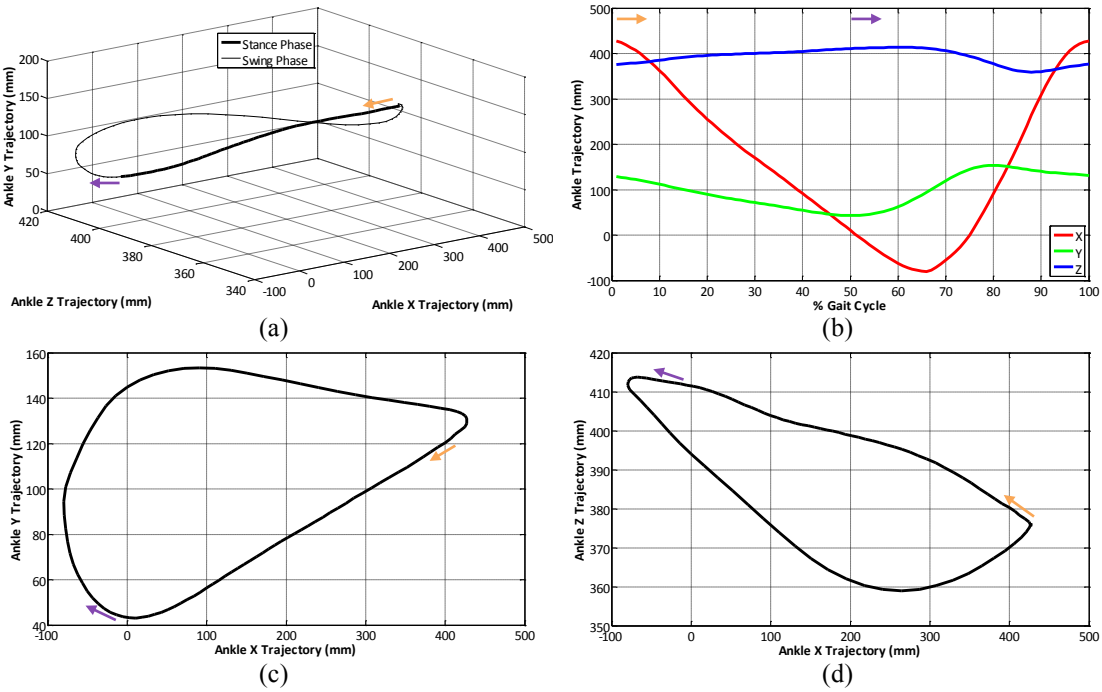

Figure 8 - Ankle trajectory: (a) 3D; (b) *X, Y* and *Z* coordinates; (c) Sagittal plane; (d) Transverse plane. The arrows depict the direction of motion.

A detailed analysis is reported for the ankle trajectory in Fig. 8. Observing simultaneously Figs. 8b and 8c it can be pointed out that at the beginning of the gait cycle, a foot touches the ground (heel-strike) and *X* and *Y* coordinates decrease till the end of stance phase. This corresponds to a backward and downward movement of the ankle. The slope in the sagittal plane is due to the 7.3° of incline of the treadmill floor. Then, the heel lifts from the treadmill and swing phase begins (toe-off). The *Y* coordinate increases till maximum ankle position during initial swing. At the same time, firstly *X* coordinate continues to decrease and then the ankle starts to move forward till the end of swing phase. After maximum *Y* coordinate, knee extends and so *Y* coordinate decreases till the heel-strike moment. Figure 8d represents the *Z* versus *X* trajectory. In the *Z* coordinate case, the stance phase only includes lateral movement. On the swing phase, both lateral and medial movements occur, corresponding to increase and decrease of *Z* coordinate, respectively. It is important to note swing phase included a larger range of *Z* coordinate since during stance phase the foot is on the treadmill and so in a more stable position. The lateral movement results from the individual adjusting his centre of gravity in order to keep balance while walking and it is consistent with the optimization strategy of gait [18]. Observing Fig. 8b and comparing the three trajectories, it is confirmed the lateral displacement is of minor value.

Figure 9a shows the knee and ankle points of 3D trajectory. Observing the planar trajectory of Fig. 9b, it can be concluded the amplitude of the horizontal movement in the ankle is much higher than the corresponding one of the knee. The amplitude of the vertical movement is also larger in the ankle, although not so different from the one of the knee. As for the lateral motion amplitude represented in Fig. 9c, it is much higher in the knee than in the ankle. As previously discussed, the minor displacement occurs for the lateral trajectory.

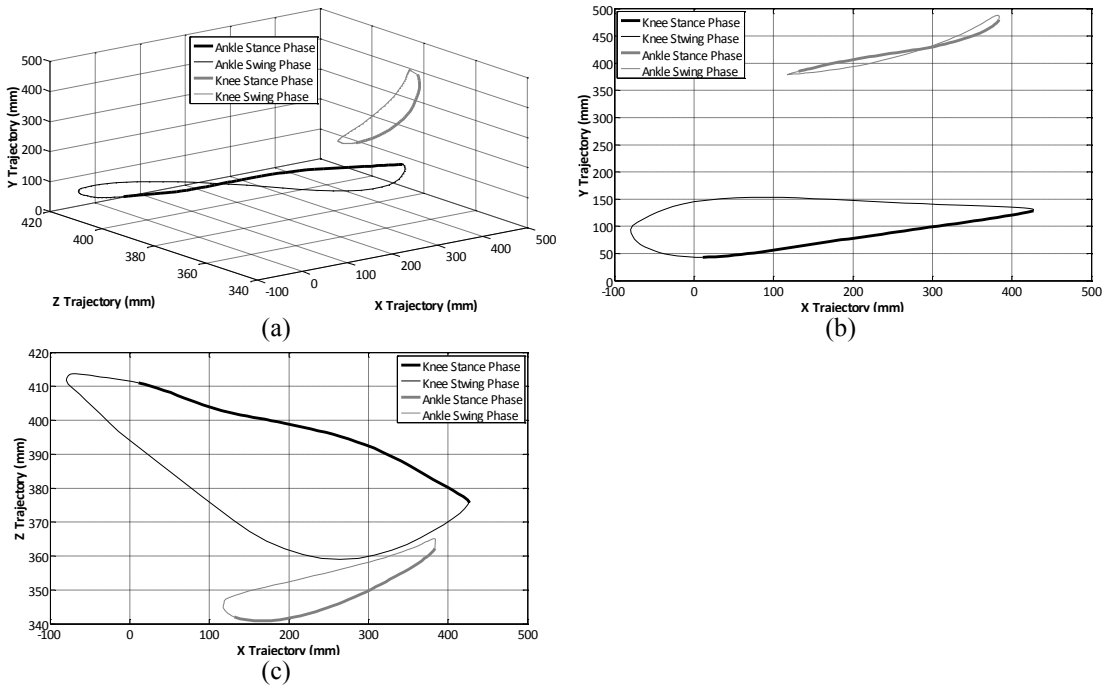

Figure 9 - Knee and ankle trajectories: (a) 3D; (b) Sagittal plane; (c) Transverse plane.

The vertical black lines in Fig. 10 represent the shank motion in sagittal plane during the gait cycle. The knee-ankle segment is considered as a rigid body and its length

should be constant, which is not verified in the present study due to the errors associated with data acquisition and the slippage of the straps.

A double pendulum model for swing and an inverse double pendulum model for stance were assumed [27]. Fig. 11 represent the θ_s in stance phase. It is clear that θ_s decrease from initial contact to the preswing, reaching 90° in maximum knee extension, i.e., in midstance. Moreover, θ_s is higher or lower than 90° if the ankle point is anterior or posterior to the knee point, respectively [21].

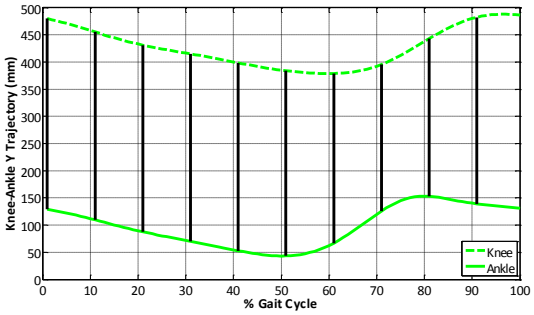

Figure 10 - Vertical ankle trajectory.

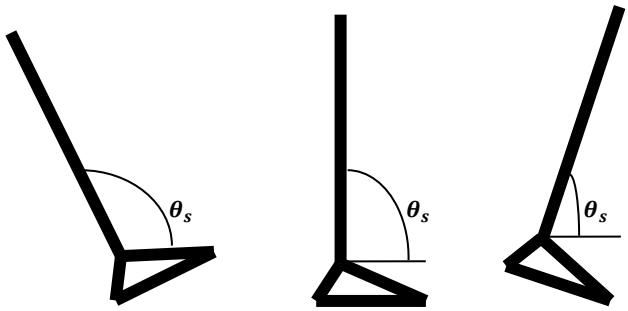

(a) (b) (c)

Figure 11 - Shank angle θs: (a) Heel-strike; (b) Midstance (θs=90°); (c) Preswing.

In Fig. 12a, heel-strike is represented by a maximum angle value (97°) and toe-off by a minimum angle value (48°).

Shank velocity is presented in Fig. 12b. It begins with a negative peak value related with heel-strike and during stance phase only negative values are observed. In the swing phase, a maximum angular velocity peak is obtained, corresponding to the midswing phase where maximum knee flexion occurs. Heel-strike and toe-off are represented by negative peaks. Periodic feature was found for the both results.

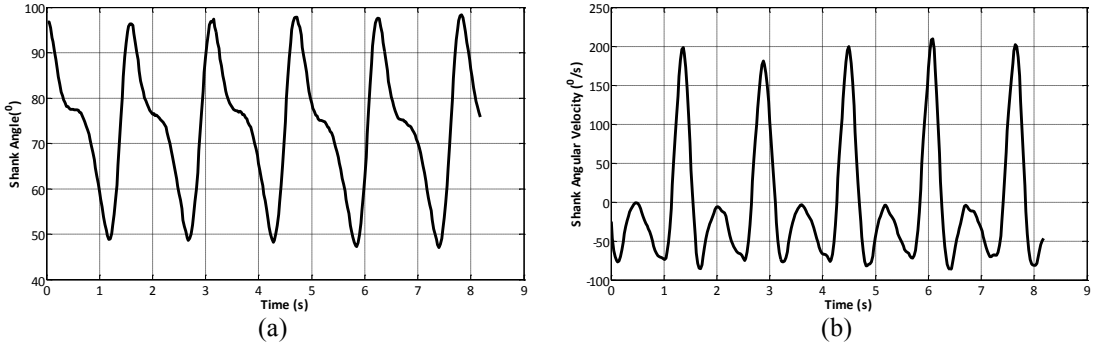

(a) (b)

Figure 12 - Gait shank results: (a) Shank angle; (b) Shank angular velocity.

Figure 13 shows the velocity and acceleration experienced during a gait cycle by the knee and ankle, respectively. Knee and ankle speed and acceleration result from the vector module of the three respective directional components.

Ankle speed (0.69 m/s) is higher than the knee one (0.38 m/s). The amplitude of the velocity components decreases in the same way for both. Horizontal velocity amplitude is the highest, followed by the vertical and at last the lateral one, which is found logical for the human walking velocity. Regarding the acceleration, mean values of 1.7 m/s^2 and 2.8 m/s^2 were found for the knee and ankle, respectively. The mean acceleration amplitude is again higher in the ankle and the directional acceleration amplitude behaves in the same way as for the ankle. Periodic pattern was found in the velocity and acceleration results of the ankle and knee gait tests.

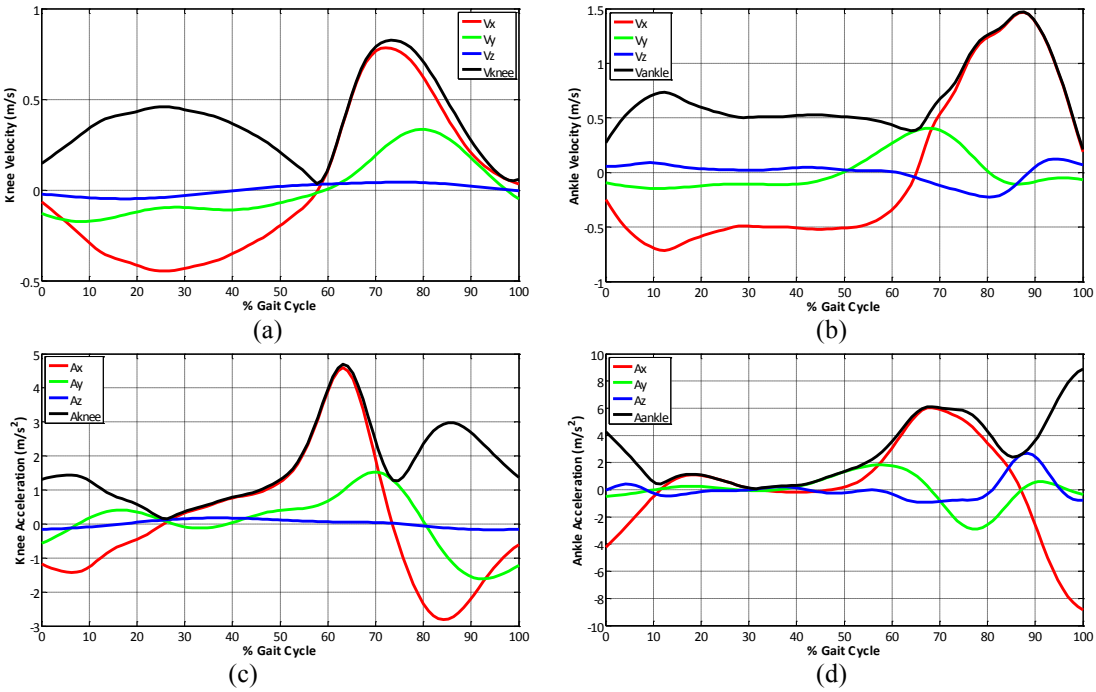

Figure 13 - Velocity and acceleration: (a) Knee velocity; (b) Ankle velocity; (c) Knee acceleration; (d) Ankle acceleration.

The matching of the physical events in the velocity and acceleration plot is not ideal due to the use of the filtering and finite-difference techniques. Nevertheless, in Fig. 13a, it is very clear a zero-crossing moment in which velocity is 0 m/s, the heel-strike moment. It corresponds to a peak acceleration of 4.7m/s^2, as shown in Fig. 13c. The same kind of event occurs in the ankle, but the corresponding values are not so high.

Table 2 shows the parameters results of a single reference test. Figure 14 represents some of these parameters. In Fig. 14a, observing the trajectory of the highest stance phase curve, it is possible to confirm the high trajectory interval between the beginning of the stance phase and the minimum vertical position, corresponding to the end of the phase. This test has the highest stance phase of the experiment, 50% of stance phase and 50% of swing phase. As for the curve with the highest swing phase, it is characterized by 63% of swing phase against 37%. In fact, in this curve the vertical minimum position is reached very early.

To demonstrate the range of the cycle length and height obtained with CaTraSys experimental tests, it is assembled in Fig. 14b the curves corresponding to the highest and lowest range of these features. Observing the black curve, it is clear a high range of

horizontal and vertical positions, corresponding to the highest cycle length and height respectively, in opposition to the grey curve.

At last, Fig. 14c presents the tests results with the highest and lowest cycle medio-lateral movement, which can be confirmed by the different range of values of the ankle lateral positions.

Table 2 - Spatiotemporal parameters for a single reference test.

Walking Distance (m)	4.06
Walking Time (s)	12.5
Number of Cycles	8
Cycle Time (s)	1.56
Cycle Cadence (cycles/s)	0.64
Stance Phase (%)	50
Swing Phase (%)	50
Cycle Height (m)	0.11
Cycle Length (m)	0.51
Cycle Medio-Lateral Movement (m)	0.06

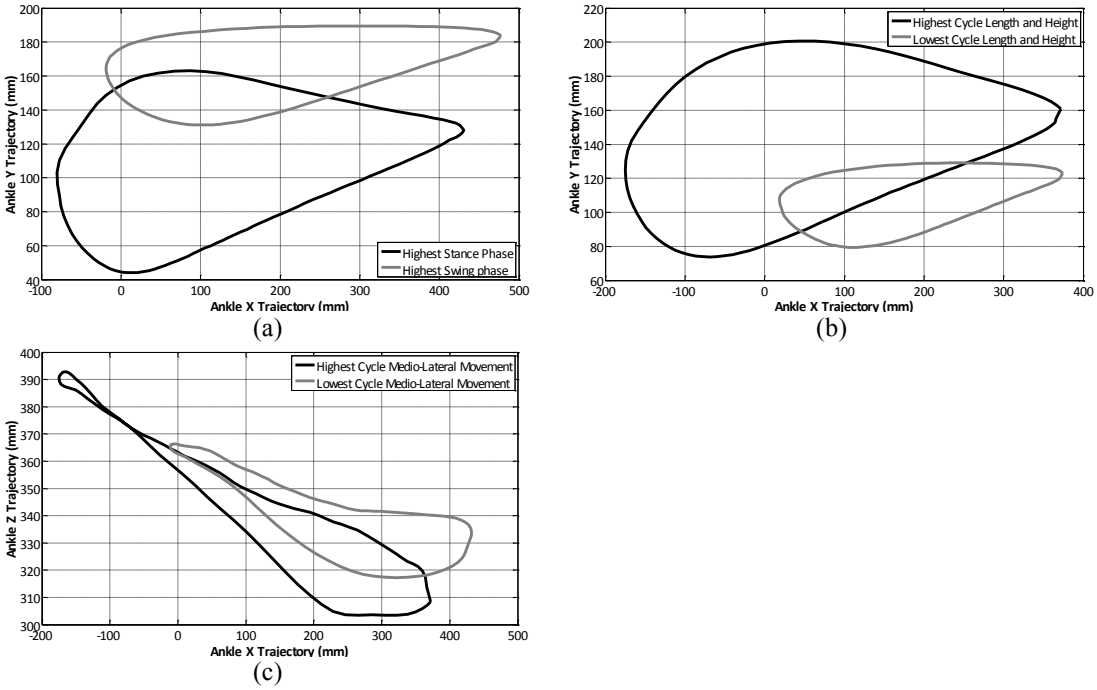

Figure 14 – Representation of the cycles with opposite values of: (a) Stance and swing phases (sagittal plane); (b) Height and length (sagittal plane); (c) Medio-lateral displacement (transverse plane).

4.1. Influence of the test conditions and anthropometric factors

Investigations had concluded human gait is highly adaptable to modifications in the mechanical demands of the current task (e.g.: different speeds or types of surfaces) [28]. One of the goals of the present work was to monitor the human gait taking into account different factors that could influence it. To this purpose four trial conditions were used: reference test, loaded test, footwear test and fast test. In order to run the comparative analysis spatiotemporal parameters were determined for all the CaTraSys tests results.

In order to compare the diverse test conditions by an inter-evaluation, the three *special* test conditions, loaded test, footwear test and fast test, were studied against the corresponding reference test. Therefore, for each subject and parameter, the difference

between the parameter value of the reference test and the *special* test condition was calculated. Important conclusions can be taken from Table 3. The behavior (signal) of the parameters was studied. A positive value means an increase of the parameter (↑), a negative one means a decrease (↓) and a zero one means the parameter was equal for the both test conditions. The cases (50) correspond to 50/50 of increment/decrement. The cases (50)↑ (or (50)↓) are the ones in which the number of cases of increment (or decrement) were superior to the zero and the decrement (or increment) cases. As for the case (40), it refers to a case in which occurred 40% of increment, 40% of decrement and 20% of non-alteration of the parameters values. In order to run an accurate analysis, it was only considered a pattern, i.e., only constituted a conclusion to the present work, if the percentage of cases was higher than 50%.

Table 3 - Values of the spatiotemporal parameters.

	Loaded Test	**Footwear Test**		**Fast Test**
		Men	**Women**	
Cycle Cadence	(62,5)↓	(80)↑	(100)↑	(100)↑
Stance Phase	(87,5)↑	(40)	(66,7)↑	(62,5)↑
Swing Phase	(87,5)↓	(40)	(66,7)↓	(62,5)↓
Cycle Height	(87,5)↑	(60)↑	(100)↓	(100)↑
Cycle Length	(62,5)↑	(60)↑	(66,7)↓	(100)↑
Cycle Medio-Lateral Movement	(50)	(60)↑	(100)↑	(50)

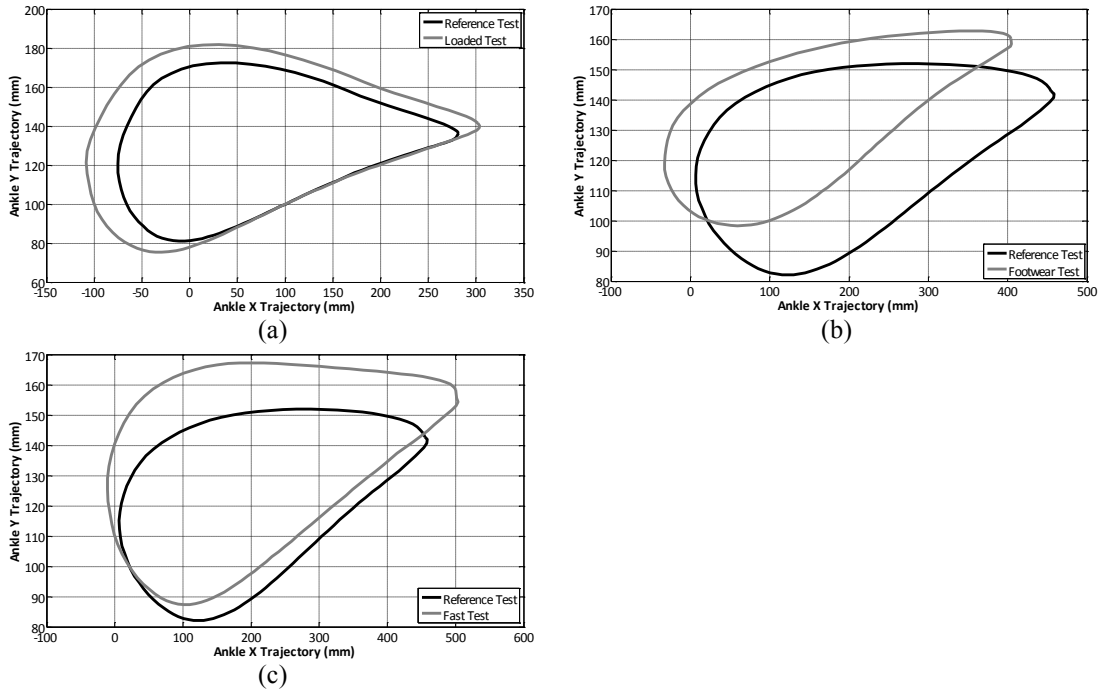

Figure 15 - Sagittal planes of a reference test versus: (a) Loaded test; (b) Footwear woman test; (c) Fast test.

In the present work, for the loading condition (see Table 3 and Fig. 15a), the cycle cadence was reduced in the majority of the cases, while stance phase, cycle height and length were increased. These values indicate that for the subject carrying load on the shoulders while walking, a slower cycle frequency occurred, the time the foot spent in the air was reduced and the amplitude of the vertical and horizontal movement was also lower.

Regarding the footwear test (see Table 3 and Fig. 15b), different conclusions were taken for men and women. From the present results, it can be concluded wearing

sportive shoes increases cycle cadence, cycle height, length and medio-lateral movement. These conclusions are not very accurate since the differences between the type of foot from the reference test (casual shoes) and the sportive shoes are probably not enough to allow its recognition from CaTraSys results.

As for the heel shoes tests results, it was adopted a quicker cadence and an increase in the stance phase. On the other hand, cycle height and length experienced a decrease and the medio-lateral movement an increment. It can be thought decreasing the cycle height and length is a defense strategy of the subject in order to maintain the stability. Wearing high heel shoes resulted in a 100% of increment in the medio-lateral motion, which is clearly justified by the instability caused by this type of shoes. Observing Fig. 16b, and comparing the curves from the reference and corresponding footwear test, it is evident an increment in all the vertical positions of the footwear curve. The modification is consequence of being a heel shoes trial.

In what refers to the fast test condition, it was observed a clear increase in the cycle cadence and stance phase as well as in the cycle height and length, as can be confirmed by Table 3 and Fig. 15c. The results are in accordance with literature. In fact, the adaptation to an increase of the walking speed is obtained with reduced cycle duration and higher cycle length, generally simultaneously [28]. The medio-lateral amplitude of movement for the fast test was 50/50 of increase/decrease relative to the reference test. Despite the present results, it was expected a major percentage of decrement. Tesio *et al* [26] observed a decrease in the medio-lateral movement of the body centre of mass with increasing speed, which is also coherent with Smeesters *et al.* [29], who concluded sideway falls are more frequent at low speeds. Although displacement of body centre of mass and medio-lateral movement are distinct concepts, it would be consistent to obtain a higher percentage of decrement in the CaTraSys results. As they do not overcome the 50%, no conclusions are inferred.

In order to give a general idea of the experimental results for different anthropometric conditions, Fig. 16 presents the sagittal trajectory of subjects with opposite values (maximum/minimum) of gender, age, height and weight, for the reference test condition.

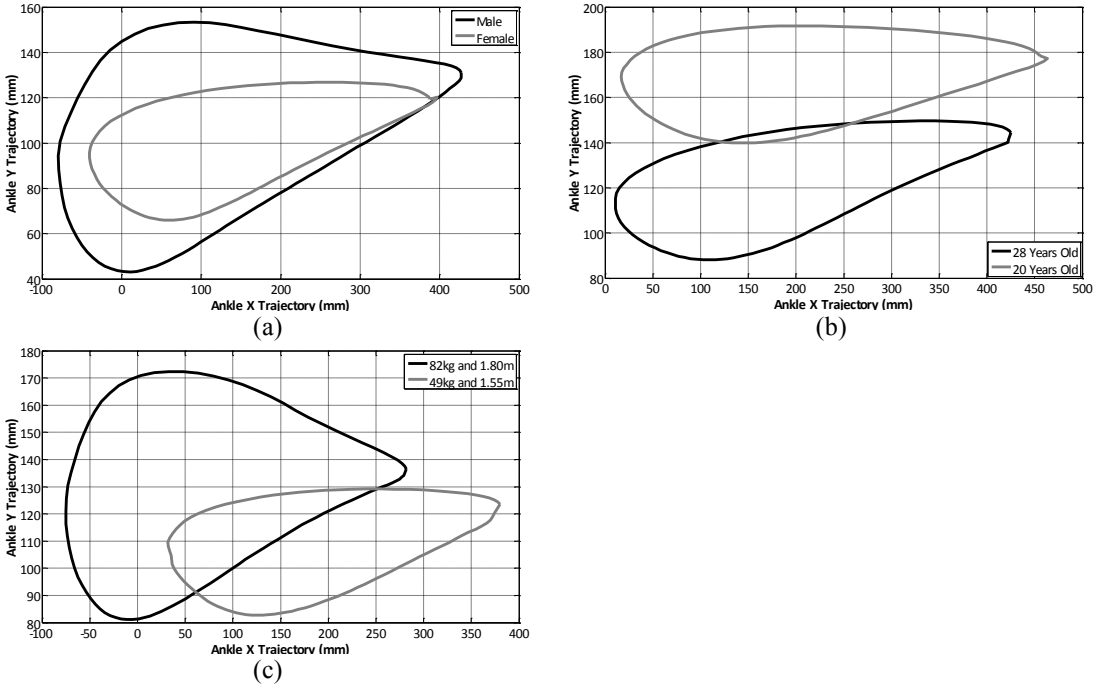

Figure 16 - Sagittal trajectories of reference tests obtained for opposite anthropometric characteristics:

(a) Gender; (b) Age; (c) Height and weight.

5. Conclusions

In the present work, the use of CaTraSys is proposed for human walking characterization. A methodology for experimental tests and data acquisition is devised. A data analysis procedure is elaborated, i.e., a novel formulation is deduced for determining kinematics of CaTraSys gait tests. Particularly, mean trajectory data of the gait assessments is determined.

Visual representation of CaTraSys results is provided through representative profiles (2D and 3D). Using the mean trajectory data, spatiotemporal parameters are computed allowing to run a quantitative analysis. Some behavior patterns for different walking conditions are found. The influence of anthropometric characteristics on the gait of the population is also studied.

The presented methods and results prove CaTraSys significance in the experimental characterization of the biomechanics of human walking, always respecting the principles of low-cost and easy operation of the proposed system.

Acknowledgments

The first author would like to acknowledge her home institution, University of Minho, for allowing her to spend a period of study at LARM in Cassino, within ERASMUS program in 2012. Tao Li, PhD student of LARM at the time, is gratefully acknowledged for the support given during the lab activity.

References

[1] T.M. Willems, D. De Clercq, K. Delbaere , G. Vanderstraeten, A. De Cock, E. Witvrouw, A prospective study of gait related risk factors for exercise-related lower leg pain, Gait & Posture 23 (2006) 91-8.

[2] T. Caderby, E. Yiou, N. Peyrot, B. Bonazzi, G. Dalleau, Detection of swing heel-off event in gait initiation using force-plate data, Gait & Posture 37 (2013) 463-6.

[3] S. Ghoussayni, C. Stevens, S. Durham, D. Ewins, Assessment and validation of a simple automated method for the detection of gait events and intervals, Gait & Posture 20 (2004) 266-72.

[4] H. Lau, K. Tong, The reliability of using accelerometer and gyroscope for gait event identification on persons with dropped foot, Gait & Posture 27 (2008) 248-57.

[5] C. Liedtke, S.A. Fokkenrood, J.T. Menger, H. van der Kooij, P.H. Veltink, Evaluation of instrumented shoes for ambulatory assessment of ground reaction forces, Gait & Posture 26 (2007) 39-47.

[6] A. De Stefano, J.H. Burridge, V.T. Yule, R. Allen, Effect of gait cycle selection on emg analysis during walking in adults and children with gait pathology, Gait & Posture 20 (2004) 92-101.

[7] T. Lee, Y. Kwon, H. Kim, Smart location tracking system using FSR (Force

Sensing Resistor), 14th International Conference on Artificial Reality and Telexistence (ICAT 2004), Coex, Korea, November 30-December 2 2004, 4 pp.
[8] E. Ottaviano, M. Ceccarelli, F. Palmucci, An application of CaTraSys, a cable-based parallel measuring system for an experimental characterization of human walking, Robotica 28 (2010) 119-33.
[9] W.M. Nunes, L.A. Rodrigues, L.P. Oliveira, J.F. Ribeiro, J.C. Carvalho, R.S. Gonçalves, Cable-based parallel manipulator for rehabilitation of shoulder and elbow movements, Proceedings of the IEEE International Conference on Rehabilitation Robotics (ICORR 2011), Zurich, Switzerland, June 29-July 1 2011, pp. 1053-1058.
[10] K. Homma, O. Fukuda, Y. Nagata, M. Usuba, Study of a wire-driven leg rehabilitation system, Proceedings of the IEEE/RSJ International Conference on Intelligent Robots and Systems (IROS 2002), Vol. 2, IEEE, Lausanne, Switzerland, September 30-October 4 2002, pp. 1451-56.
[11] I. Díaz, J.J. Gil, E. Sánchez, Lower-limb robotic rehabilitation: literature review and challenges, Journal of Robotics 2011 (2011) 1-11.
[12] M. Ceccarelli, The historical development of CaTraSys, a cable system. Explorations in the History of Machines and Mechanisms, Proceedings of the HMM2012, T. Koetsier, M. Ceccarelli (Eds.), Springer, Amsterdam, Netherlands, May 7-11 2012, pp. 365-79.
[13] H. Iida, T. Yamamuro, Kinetic analysis of the center of gravity of the human body in normal and pathological gaits, Journal of Biomechanics 20 (1987) 987-95.
[14] celesco™, Linear and rotary measurement solutions, PT101 cable-extension tranducer, 2012, 291 pp.
[15] LAUMAS®, Load cells and mounting kits, SA tension (compression) load cells, 2013, 91 pp.
[16] LAUMAS®, Electronic instrumentation, TPS Analog weight transmitter, 2013, 150 pp.
[17] National Instruments™, NI USB-621x specifications, 2009, 16 pp.
[18] T. Li, M. Ceccarelli, An experimental analysis of human straight walking, Frontiers of Mechanical Engineering 8 (2013) 95-103.
[19] V. Macellari, C. Giacomozzi, Multistep pressure platform as a stand-alone system for gait assessment, Medical & Biological Engineering & Computing 34 (1996) 299-304.
[20] M. Kutz, Biomedical engineering and design handbook, Vol. 1, 2nd ed., The McGraw-Hill Companies, Inc., 2009, 688 pp.
[21] D.A. Winter, Biomechanics and motor control of human movement, 3rd ed., John Wiley & Sons, Inc., 2005, 325 pp.
[22] V. Klika, Biomechanics in applications, InTech, 2009, 408 pp.
[23] I. Stancic, T.G. Supuk, M. Bonkovic, New kinematic parameters for quantifying irregularities in the human and humanoid robot gait, International Journal of Advanced Robotic Systems 9 (2012) 01-08.
[24] T. M. Owings, M.D. Grabiner, Step width variability, but not step length variability or step time variability, discriminates gait of healthy young and older adults during treadmill locomotion, Journal of Biomechanics 37 (2004) 935-8.
[25] M. Whittle, Gait analysis: an introduction, 4th ed., Butterworth-Heinemann, 2007, 255 pp.
[26] L. Tesio, V. Rota, C. Chessa, L. Perucca, The 3D path of body centre of mass during adult human walking on force treadmill, Journal of Biomechanics 43

(2010) 938-44.
[27] A. Salarian, H. Russmann , F.J. Vingerhoets, C. Dehollain, Y. Blanc, P.R. Burkhard, K. Aminian, Gait assessment in Parkinson's disease: toward an ambulatory system for long-term monitoring, IEEE Transactions on Biomedical Engineering 51 (2004) 1434-43.
[28] A. Pepin, K.E. Norman, H. Barbeau, Treadmill walking in incomplete spinal-cord-injured subjects: 1. Adaptation to changes in speed, Spinal Cord 41 (2003) 257-70.
[29] C. Smeesters, W.C. Hayes, T.A. McMahon, Disturbance type and gait speed affect fall direction and impact location, Journal of Biomechanics 34 (2001) 309-17.